

Modeling and detection of the prepared tool edge radius

Science Progress

2020, Vol. 103(3) 1–20

© The Author(s) 2020

Article reuse guidelines:

sagepub.com/journals-permissions

DOI: 10.1177/0036850420957903

journals.sagepub.com/home/sci**Zhao Xuefeng**¹, Li Hui, He Lin and Tao Meng

Mechanical Engineering College, Guizhou University, Guiyang, China

Abstract

Introduction: High-speed and high-efficient machining is the inevitable development direction of machining technology. The tool edge preparation can improve the life, cutting performance, and surface quality of a tool and help to achieve high-speed and efficient machining. Therefore, precise modeling and detection of the micron-level contour of a tool edge are crucial for edge preparation. The aim of this study is to provide the model and detect method of the prepared tool edge radius.

Methods: The mathematical model of the milling tool trajectory is established through the Matlab. The material removal model by single abrasive particle is established based on the energy conservation principle and energy absorption theory. The material removal model by multiple abrasive grains on the cutting tool edge is constructed using the statistical methods. The mathematical model of the edge radius is established through the geometrical relationship. The milling edge preparation contour detection system is setup based on the machine vision principle through LabVIEW software. Finally, the edge radius at different process parameters is determined by the mathematical model and detection system, and the results are compared with the results of the scanning electron microscopic measurement (SEM).

Results: Through the Comparison and analysis of the edge radius measured by the SEM and calculated by the proposed model. The maximum error between the analytical results and SEM measurements is 11.18 μm , while the minimum error is 0.07 μm . Through the comparison and analysis of the edge radius measured by the SEM and the edge detection system. The maximum difference between the two methods is 2.71 μm , and the minimum difference is 0.31 μm . The maximum difference in percentage is 9.2%, and the minimum difference in percentage is 1.2%.

Discussions: The edge preparation mechanisms of a single particle and multiple particles on the tool edge are explained. A mathematical model of the edge radius is established, which provides a basis for a deeper understanding of the edge preparation effect. Based on the machine vision principle, the prepared tool micron-level edge detection method is proposed. The histogram specification method, median filtering, multi-threshold segmentation method, and Canny edge detection operator are adopted to obtain the edge contour. The comparison result shows that the mathematical model of the edge radius is accurate, and the proposed tool edge detection method is

Corresponding author:

Zhao Xuefeng, Mechanical Engineering College, Guizhou University, Guiyang 550025, China.

Email: zxf801112@163.com

Creative Commons Non Commercial CC BY-NC: This article is distributed under the terms of the Creative Commons Attribution-NonCommercial 4.0 License (<https://creativecommons.org/licenses/by-nc/4.0/>)which permits non-commercial use, reproduction and distribution of the work without further permission provided the original work is attributed as specified on the SAGE and Open Access pages (<https://us.sagepub.com/en-us/nam/open-access-at-sage>).

feasible, which lays the foundation for edge preparation and realization of high-speed and high-efficient machining.

Keywords

Edge preparation, edge radius, drag finishing, modeling, machine vision

Introduction

High-speed and high-efficient machining is the inevitable development direction of machining technology. The tool edge preparation can improve the process stability, tool life, and surface quality changing the micro-contour edge and micro-morphology, which helps to achieve high-speed and high-efficient machining. The precise modeling and detection of the micron-level contour of a tool edge are crucial for edge preparation.¹

Different edge preparation methods are based on different mechanisms. The tool edge preparation by using abrasive particles has the characteristics of good repeatability, high quality, and low cost, and it is the most preferred edge preparation method at present. In this edge preparation method, the tool edge preparation is achieved through relative movement of the tool and abrasive particles, such as diamond, cubic boron nitride (CBN), brown alumina, and SiC particles.² So far, not much research has been conducted on the action mechanism of abrasive particles on the workpiece surface. The impact wear due to a single abrasive grain,³ multiple particles,⁴ particles between the tool and a chip,⁵ abrasive water jets,⁶ and semi-fixed abrasive particles⁷ have been studied. The effects of the affecting parameters of abrasive particles, such as type, size, and velocity, on the surface have been studied experimentally. However, there is less published research on the action mechanism of dispersed solid abrasive particles on the workpiece surface.

The influence of edge preparation parameters on the edge radius has been mainly studied experimentally. However, the edge preparation mechanism has not been thoroughly studied yet. Uhlmann et al.⁸ used the drag finishing method for edge preparation of micro-cutting tools, the relationship between the preparation time and the edge radius was investigated, and the influence law that relates the edge radius and tool wear was studied through the cutting experiments, and it was concluded that establishing a proper tool edge preparation could reduce tool wear. Barletta et al.⁹ used two kinds of abrasive particles with different sizes and experimentally found that the planetary motion polishing method assisted by an abrasive bed could achieve a better polishing effect than the centrifugal disk method in a relatively short time. Sooraj and Radhakrishnan¹⁰ conducted a polishing experiment on the drag finishing equipment assisted by an abrasive bed, and the influence of the technological variables on the polishing effect was studied. The surface roughness was reduced to 0.0267 μm under the optimum operating conditions.

Due to the micron level of a tool edge, there have been a few studies on the preparation edge detection. Yeong adopted the subpixel boundary detection and proposed a batch detecting method of the cutting edge radius. The error was reduced by 3% compared to the Alicona 3D surface profiler.¹¹ Ratnam proposed an

accurate machine vision-based method for obtaining the edge radius. The maximum error was reduced by 3.7% compared to the contour projector test results.^{12,13} Most tool detectors are based on machine vision. A variety of tool parameters, including the rake angle, front angle, arc, and step surface, can be measured by the UTS Tool Detection Equipment PG-1000 series detector. The machine vision-based tool parameter measuring instrument has been developed by the Alfred Zoller company, German. The repeated measurement accuracy reached a few microns, and this instrument has been industrialized.¹⁴

The forming mechanism and detection of the prepared edge are very complex. The drag finishing method is adopted in this study. The mathematical model of the milling tool motion trajectory is developed based on the characteristics of this method. The mathematical model of material removal by a single abrasive particle impacting on the cutting tool edge is based on the energy conservation principle and energy absorption theory. The mathematical model of material removal by multiple particles impacting on the tool edge is developed using the statistical method while that of the edge radius is based on geometrical methods. In this work, the hardware system of the milling tool edge detection system is established using the machine vision. The software system, including the image filtering module, image segmentation module, and Canny edge detection module, is developed using the LabVIEW software. The detection method of a micron-level edge radius is proposed. The suitability of the proposed modeling method for the dispersed solid abrasive acting on a tool edge and the effectiveness in the micron-level edge radius detection are verified by comparison with the edge radius measured by the scanning electron microscope (SEM), which provides the basis for understanding the wear mechanism of abrasive particles acting on the workpiece surface and optimization of the tool edge preparation process.

Tool edge radius modeling

Tool edge preparation method

In this study, the drag finishing method is used for tool edge preparation. Besides for edge preparation, the drag finishing method is used for workpiece polishing. A dispersed solid abrasive consisted of walnut powder, brown corundum particles, and silicon carbide particles mixed in a certain proportion is packed in the container. Multiple tools are mounted on the spindle and they can move along a two-stage planetary trajectory in the dispersed solid abrasive particles. In the drag finishing method, each tool undergoes both rotation and revolution movements. The tool edge is prepared by the continuous action of the dispersed solid abrasive particles, thus removing micro-level defects and ensuring efficient and uniform edge preparation. The milling tool moves along a predetermined trajectory while the movements of the dispersed solid abrasive particles are random. Therefore, the action of the dispersed solid abrasive particles on the cutting tool edge has a very complex behavior, which requires thorough studying.

In the edge preparation process, the tool performs a two-stage planetary motion. The simplified illustration of the two-stage planetary motion of the tool is displayed in Figure 1. In Figure 1, the tool rotates around axis O_3 while axis O_3 revolves around axis O_2 , and axis O_2 simultaneously revolves around axis O_1 . Thus, the rotation and revolution of all the tools are achieved. The mathematical model of the milling tool tooth movement trajectory is given by equation (1), and it is shown in Figure 2.

$$\begin{aligned} x &= R_1 \times \sin(\omega_1 t) + R_2 \times \sin(\omega_2 t) + R_3 \times \sin(\omega_3 t) \\ y &= R_1 \times \cos(\omega_1 t) + R_2 \times \cos(\omega_2 t) + R_3 \times \cos(\omega_3 t) \end{aligned} \quad (1)$$

where, ω_1 denotes the rotational speed of axis O_2 around axis O_1 , ω_2 denotes the rotational speed of O_3 around O_2 , ω_3 denotes the rotational speed of the milling tool tooth around O_3 ; R_1 denotes the rotational radius of O_2 around O_1 , R_2 denotes the rotational radius of O_3 around O_2 , and R_3 denotes the tool rotation radius.

Material removal by single abrasive particle

The edge preparation process passivates the sharp and non-smooth edge of cutting tools into a smooth arc of a certain shape. The edge contour of a tool is very complex, and the tool edge size is of the order of microns. At present, the edge radius of the arc contour is the evaluation criteria of the edge morphology of prepared tools. The effects of edge preparation parameters on the edge radius and the effect of edge radius on the cutting performance are studied. Thus, in order to obtain the optimum size of the tool edge and effective edge preparation, the mathematical model of the edge radius needs to be established, and the effects of the edge preparation parameters on the edge radius need to be investigated.

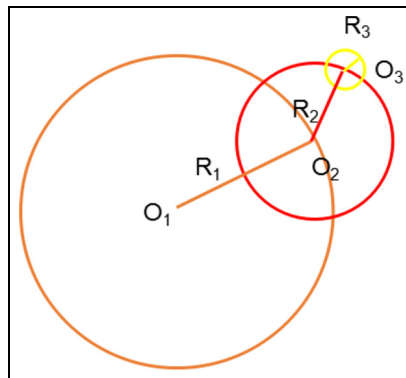


Figure 1. Simplified illustration of the two-stage planetary motion during the edge preparation process.

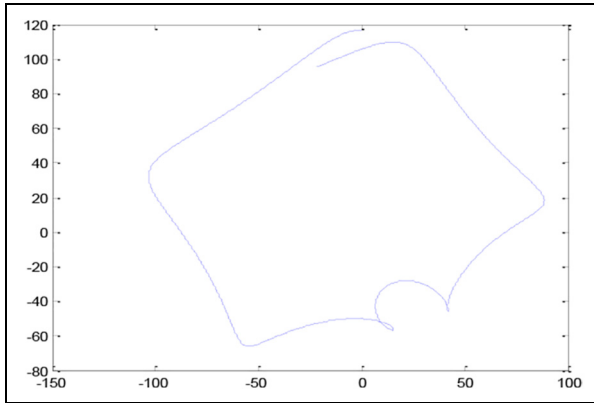


Figure 2. The trajectory of the milling tool motion.

The impact of abrasive particles on the workpiece surface can lead to the plastic deformation and indentation of the workpiece surface. When multiple particles impact the workpiece surface repeatedly, the pitting is caused by erosion, and the indentations are generated by the impacts overlap. After a certain period of time, the workpiece surface becomes smooth, which represents the workpiece polishing mechanism. When a two-stage planetary motion of the milling tool is carried out in the barrel containing abrasive particles, the impacts of the abrasive particles cause minute amount of material to be removed from the surface of the milling tool edge. With the increase in the edge preparation time and change in the tool trajectory, the abrasive particles along the trajectory impact the cutting tool edge continuously. The volume of material removal from the cutting tool edge increases, and finally, the sharp edge is completely removed, thus forming a smooth circular arc of a certain shape and completing the uniform edge preparation of the cutting tool. In this study, the material removal mechanism of a single abrasive particle acting on the cutting tool edge is used to develop a material removal volume model of multiple abrasive particles acting on the cutting tool edge using the statistical method, and the mathematical model of the edge radius of the prepared tool is developed using the geometry method.

As mentioned above, the material removal behavior of a dispersed abrasive on the cutting tool edge is very complex. In order to simplify the model of the abrasive action on the cutting tool edge, the following assumptions are made:

1. Abrasive particles are spherical and of the same size.
2. Section shape of the cutting tool edge is triangular.
3. After the edge preparation, the tool edge has a shape of a regular arc.

The energy conservation principle and energy absorption theory are adopted for developing the material removal model of a single abrasive particle impacting the

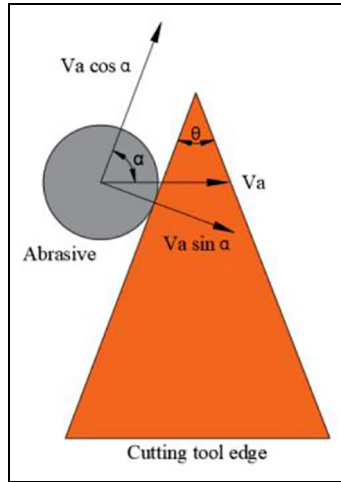


Figure 3. The impact of a single abrasive particle on the cutting tool edge.

cutting tool edge. The difference between the impact kinetic energy and the spring back kinetic energy of a single abrasive particle, that is, the energy loss, is used for the deformation of the cutting tool edge, according to the energy absorption theory.

When an abrasive particle having a diameter d_a and a mass m_a impact the cutting tool edge at an impact velocity V_a and at an impact angle α , the impact velocity V_a of the abrasive particle on the cutting tool edge can be decomposed into two components, tangential velocity $V_a \cos \alpha$ and normal velocity $V_a \sin \alpha$. The impact of a single abrasive particle on the cutting tool edge is presented in Figure 3. The impact depth of a single abrasive particle on the cutting tool edge, denoted as h , is presented in Figure 4.

When a single abrasive particle impinges on the cutting tool surface at speed $V_a \sin \alpha$, the kinetic energy of initial impact E_i and the rebound kinetic energy E_r can be respectively expressed by:

$$E_i = \frac{1}{2} m_a (V_a \sin \alpha)^2 \quad (2)$$

$$E_r = \frac{1}{2} m_a (V_a e_p \sin \alpha)^2 \quad (3)$$

where e_p represents the restitution coefficient of a single abrasive grain having a mass m_a .

Considering that the kinetic energy loss is transformed into the deformation energy, the restitution coefficient can be calculated as a ratio of the rebound velocity to the impingement velocity.

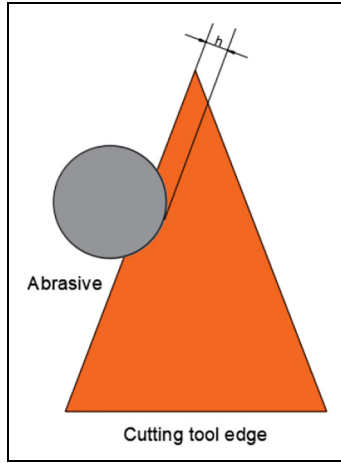


Figure 4. The impact depth of a single abrasive particle on the cutting tool edge.

Based on the theoretical models developed by Johnson, the restitution coefficient of the abrasives can be expressed as a function of the impingement velocity, mechanical properties of the work material, abrasive size, and abrasive density,¹⁵ which is given by:

$$e_p = \frac{1.7(p_y)^{\frac{5}{8}}}{(V_a)^{\frac{1}{4}}(\rho_a)^{\frac{1}{8}}(E^*)^{\frac{1}{2}}} \quad (4)$$

where p_y denotes the limiting value of the contact stress, ρ_a denotes the abrasive density, and E^* denotes the equivalent elastic modulus at the contact interface, and it is expressed as follows:

$$\frac{1}{E^*} = \frac{1 - \nu_a^2}{E_a} + \frac{1 - \nu_w^2}{E_w} \quad (5)$$

where E and ν denote the elastic modulus and Poisson's ratio respectively; suffix a stands for abrasive, and suffix w stands for a tool.

The impact force of a single abrasive particle on the cutting tool edge denoted as F facilitates its penetration into the tool edge surface till the impact depth h . The work done by the contact force F via penetrating through the material till the impact depth h can be referred as the elastic work, and its results in erosion, which is expressed as:

$$W = \frac{1}{2}Fh \quad (6)$$

The impact force F can be expressed as a function of the contact area between the abrasive particles and cutting tool edge and the Brinell hardness of the cutting tool material, which is expressed as:

$$F = (\pi d_a h) H_w \quad (7)$$

The depth of the impact wear can be derived based on the energy conservation principle according to which the loss in kinetic energy is transformed into the deformation energy of the cutting tool; thus, the penetration depth h can be calculated as follows:

$$h^2 = \frac{m_a V_a^2 \sin^2 \alpha (1 - e_p^2)}{\pi d_a H_w} \quad (8)$$

The material removed by a single abrasive particle from the cutting tool edge surface is regarded to be in the form of an approximately spherical segment with a radius r_a and height h . Therefore, the removed material volume corresponding to the action of a single abrasive particle on the cutting tool edge surface is the volume of a spherical segment, which is calculated by:

$$V_w = \pi h^2 \left(r_a - \frac{h}{3} \right) \quad (9)$$

Material removal by multiple abrasive particles

Using the previously presented material removal model of a single abrasive particle on the cutting tool edge, the material volume removed by multiple abrasive particles on the cutting tool edge can be obtained when the number of abrasive particles is known. In this study, the quantity of abrasive particles is considered to be the abrasive particles swept by the cutting tool during the edge preparation process.

The length of the cutting tool trajectory in the abrasive barrel during the edge preparation time that is denoted as T can be calculated by:

$$S = \int_0^T \sqrt{[x'_c(t)]^2 + [y'_c(t)]^2} dt \quad (10)$$

where $x_c(t)$ and $y_c(t)$ denote functions of the preparation time that represent the moving locus of the cutting tool edge.

During the edge preparation time T , the differential form of the material volume removed from the tool as it sweeps through the abrasive barrel can be expressed as:

$$dV_s = L l_c dS \quad (11)$$

where L denotes the length of the milling tool, and l_c represents the thickness of the milling tool edge.

The total number of the abrasive particles that impact the cutting tool edge during the edge preparation time T can be expressed as:

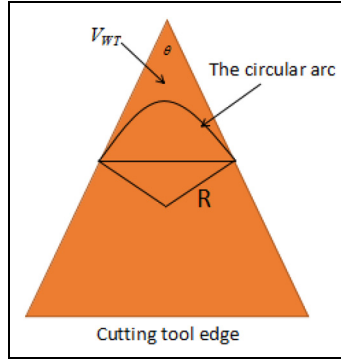


Figure 5. The relation between the removed material volume and edge radius.

$$n_T = n_v V_s \quad (12)$$

where n_v denotes the number of the elastic abrasive grains per unit volume in the abrasive barrel, and it can be expressed as a ratio of the stacking density ρ_f over the mass of a single elastic abrasive:

$$n_v = \frac{\rho_f}{m_a} \quad (13)$$

The stacking density ρ_f of the abrasive particles in the abrasive barrel is obtained from the radius of the abrasive barrel, the total mass of abrasive particles, and their accumulation height. Assume abrasive particles of mass M are poured into the barrel of radius R_s , and the stacking height of the abrasive particles is H_f . Then, the stacking density of the abrasive particles can then be obtained by:

$$\rho_f = \frac{M}{\pi R_s^2 H_f} \quad (14)$$

Therefore, during the edge preparation time T , the total volume of material removed by multiple abrasive particles impacting the cutting tool edge can be expressed as:

$$V_{wT} = n_T V_w \quad (15)$$

Mathematical model of cutting tool edge radius

The relationship between the edge radius of the cutting tool denoted as R and the total volume of removed material is shown in Figure 5.

Therefore, the mathematical model of the edge radius of the cutting tool for an edge preparation time T can be expressed as:

$$R^2 = \frac{V_{\omega T}}{\left\{ \frac{\sin^2\left(\frac{180^\circ-\theta}{2}\right)}{\tan\left(\frac{\theta}{2}\right)} + \frac{\sin(180^\circ-\theta)}{2} - \left(\frac{180^\circ-\theta}{360^\circ}\right)\pi \right\} L} \quad (16)$$

Tool edge radius detection system

System hardware

Following the basic principles of machine vision and micron-level edge detection accuracy requirements, a tool preparation edge detection system, including the optical imaging system, mechanical system, and software system, is designed.

The optical imaging system mainly includes the OPT-RI5030-B ring light source, FL2G-50S5M/C CCD (Charge Coupled Device) industrial camera, OPT-CC4M-65 telecentric lens, and the glass material calibration plate. The theoretical imaging field is $2.2 \text{ mm} \times 1.65 \text{ mm}$. Due to the reasonable collocation of the industrial camera and telecentric lens, the theoretical imaging accuracy is $0.89 \mu\text{m}$. The image acquisition effect is improved by using the backlight illumination and low-angle ring light source, which helps to achieve accurate edge detection of a prepared tool.

The fasten and specific movements of the hardware part are achieved in the mechanical system. The prepared tool edge detection system is shown in Figure 6. The mechanical system meets the optical imaging system principles, lighting theory, and system calibration principle. It also meets the requirements of taking photos of the milling tools with different diameters and different edges of the same milling tool. The lead screw guide 1, 2, 3 can realize the relative movement between the camera and milling tool in the three direction. The swallow grooves slide 4 can realize the fine adjustment in the X direction. The relative motion between the milling tool 12 and the ring light source 7 in the Z direction through the pulling rod 5. While the circular crossbar 6 can realize the motion in the X direction. The rotation of the milling tool can be achieved through the constant alignment coaxiality meter. The calibration plate gripper 8 can realize the calibration of the tool edge.

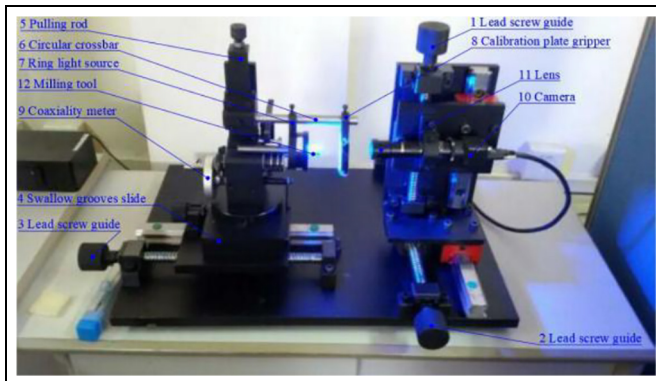


Figure 6. The tool edge preparation detection system.

The workflow of the prepared tool edge detection system is as follows. First, a real, less-noisy image is obtained under even and stable illumination provided by the ring light source to the milling tool edge and calibration plate. Then, the milling tool edge images and the calibration plate images are captured by industrial cameras and telecentric lenses. Finally, the software system based on the LabVIEW software is developed to process the images. The milling tool edge is extracted, and the micro-level edge contour is accurately detected by this system.

Image processing algorithm

The image acquisition process is inevitably disturbed by various noises. The collected images include noise signals, which affects the extraction accuracy of image contours. Therefore, the tool edge image needs to be processed in order to obtain an accurate radius. The image processing method is as follows.

Histogram specification method. The image enhancement technology refers to the enhancement of the whole or local characteristic purposely. The noise signal is suppressed. The difference between the target signal and the surrounding environment is enlarged. The recognizable effect of the human and the machine on the target signal is improved. The spatial domain method directly changes the gray values of all pixels in the image by a certain method to enhance the target characteristics of the image. The histogram specification method is to enhance the contrast of the image signal in a certain gray-value range to obtain a special histogram, which realizes the image enhancement effect.

Assume r , z , u , and v are random variables of a continuous image; $Pr(r)$ denotes the probability density function of the original gray image; $Pz(z)$ denotes the probability density function of the desired gray image. The two probability density functions are histogram equalization as follows:

$$u = T(r) = \int_0^r P_r(w)dw \quad (17)$$

$$v = G(z) = \int_0^z p_z(t)dt \quad (18)$$

$$z = G^{-1}(v) \quad (19)$$

The histogram specification method does not change the uniform density of an image. Therefore, the uniform density of $Pr(r)$ and $Pz(z)$. v in inverse processes can be replaced by u .

$$z = G^{-1}(u) = G^{-1}[T(r)] \quad (20)$$

where Z denotes the desired probability density function.

Median filtering algorithm. The median filtering is a field calculation method commonly used in the image processing field, and it represents a nonlinear filtering denoising method. The median filtering can eliminate or weaken the high-frequency components and impulse noise on target signal interference to protect the image contour and other useful information and reduce the distortion of the effective signal. The image pixel represents a two-dimensional discrete function. The special field of 3×3 pixels square window. Nine pixels in the window are sorted according to the gray level. The gray value of the average gray level in the sequence is taken as the gray value of the specific pixel point. The filtering effect is expressed as follows:

$$f(i, j) = Med_A\{g(i, j)\} \quad (21)$$

where A denotes the window, and $\{g(i, j)\}$ represents a two-dimensional data sequence.

Multi-threshold segmentation method. The multi-threshold segmentation method is a simple threshold segmentation. Given two or more threshold values, different local areas are segmented according to the gray level. Namely, in the case of two threshold values, all gray pixel values between the two thresholds are replaced by a specific gray value P . Assume the gray image value at point (x, y) is $g(x, y)$, and the gray image value after the segmentation is $f(x, y)$; and T_1 and T_2 are the selected threshold values; P_1 , P_2 , and P_3 denote the specific gray values after substitution. The formula is as follows:

$$F(x, y) = \begin{cases} P_1 & g(x, y) < T_1 \\ P_2 & T_1 \leq g(x, y) \leq T_2 \\ P_3 & g(x, y) > T_2 \end{cases} \quad (22)$$

The image is divided into three regions corresponding to P_1 , P_2 , and P_3 ; if P_1 equals P_3 , the image is divided into two regions.

Edge radius detection algorithm

Once a tool edge image is filtered and segmented, the edge profile extraction can be conducted. The extraction method of the milling tool edge profile is important to the edge detection system. In this work, the Canny edge detection operator is adopted to extract the milling tool edge profile. The Canny edge detection operator uses a two-dimensional Gaussian filter function for image filtering to eliminate the image noise. The first-order partial derivative finite difference method is used to obtain a smoothed gradient vector. The calculated gradient amplitude is non-maximal value suppressed. The edge is connected through the dual-threshold algorithm.^{16,17}

Gaussian filter. The Gaussian function is filtered by applying the first derivative, which is expressed as follows:

$$G(x, y) = \frac{1}{2\pi\delta^2} \exp\left(-\frac{(x^2 + y^2)}{2\delta^2}\right) \quad (23)$$

The gradient vector corresponding to the Gaussian function is as follows:

$$\nabla G(x, y, \delta) = \begin{bmatrix} \frac{\partial G}{\partial x} \\ \frac{\partial G}{\partial y} \end{bmatrix} \quad (24)$$

The two one-dimensional filters are split as follows:

$$\frac{\partial G}{\partial x} = kx \exp\left(-\frac{x^2}{2\delta^2}\right) \exp\left(-\frac{y^2}{2\delta^2}\right) \quad (25)$$

$$\frac{\partial G}{\partial y} = ky \exp\left(-\frac{y^2}{2\delta^2}\right) \exp\left(-\frac{x^2}{2\delta^2}\right) \quad (26)$$

The function is convoluted with the two filter templates above:

$$P_x = \frac{\partial G(x, y, \delta)}{\partial x} * g(x, y) \quad (27)$$

$$P_y = \frac{\partial G(x, y, \delta)}{\partial y} * g(x, y) \quad (28)$$

where coefficient k is constant. The standard deviation σ of the Gaussian function is used to control image smoothness. The smaller the value of σ is, the higher the image edge location accuracy and the smaller the signal-to-noise ratio are, and vice versa.

Gradient amplitude and direction angle calculation. The gradient vector is calculated using a first-order finite-difference approximation in a 2×2 field. The partial derivatives in the x and y directions denoted as $Q_x(i, j)$ and $Q_y(i, j)$ are respectively calculated by:

$$Q_x(i, j) = (g(i + 1, j) - g(i, j) + g(i + 1, j + 1) - g(i, j + 1))/2 \quad (29)$$

$$Q_y(i, j) = (g(i, j + 1) - g(i, j) + g(i + 1, j + 1) - g(i + 1, j))/2 \quad (30)$$

The magnitude $M(i, j)$ and the direction $\theta(i, j)$ are respectively obtained by:

$$M(i, j) = \sqrt{Q_x(i, j)^2 + Q_y(i, j)^2} \quad (31)$$

$$\theta(i, j) = \arctan \frac{Q_y(i, j)}{Q_x(i, j)} \quad (32)$$

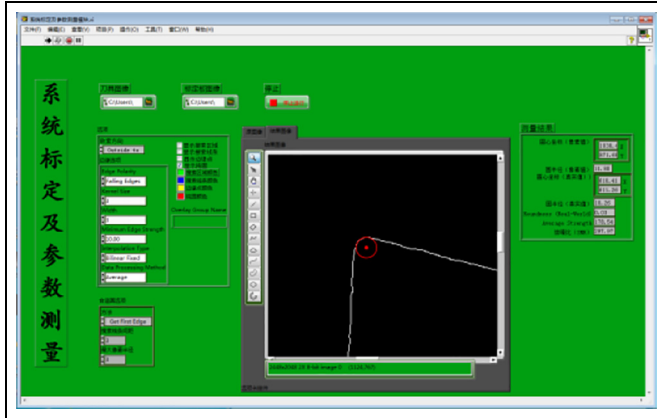


Figure 7. The tool edge radius detection interface.

Amplitude $M(i, j)$ reflects the image edge strength, and direction $\theta(i, j)$ reflects the edge direction of the image.

Non-maximal suppression. The larger the gradient magnitude image of array $M(i, j)$ is, the larger the gradient value of the image at the corresponding point is. However, this does not mean that it is the image marginal point. Since the above calculation is to find the abrupt point and change the abrupt point into the local maximum value of magnitude $M(i, j)$ only by narrowing the roof ridge in the amplitude image, it is possible to determine whether it is the image edge point by keeping the point with the largest local change in amplitude. This method is called the non-maximal suppression, and it can suppress the amplitude of all non-ridge crests and get a thinned image edge.

Double-threshold detection. The typical way for reducing the fake edge is to compare the gradient magnitude to a selected threshold value T . Also, the gray value of a pixel whose gray value is below the threshold value T is zeroed. The double-threshold method is proposed for the Canny edge detection. First, the high threshold value T_h is determined, which is calculated by the cumulative statistical histogram. Then, the low threshold T_l is determined, and its value is $T_l = 0.4T_h$. A pixel is the edge point if the gradient amplitude is greater than the high threshold T_h , so a pixel is not the edge point if the gradient amplitude is lower than the low threshold T_l , and the pixel is not necessarily the edge point if $T_h \geq T \geq T_l$. Further, a pixel is an edge point if its adjacent eight pixels have a pixel amplitude greater than the high threshold T_h ; otherwise, the pixel is not an edge point.

Therefore, the milling tool edge profile is obtained by extraction using the Canny edge detection operator.

As mentioned previously, the software of the prepared tool edge detection system is based on the LabVIEW software. The tool edge points are extracted by the image process method and Canny edge detection algorithm. The edge points are

Table 1. Main experimental parameters.

Parameter	Silicon carbide	Milling tool	Brown alumina
Poisson's ratio	0.14	0.3	0.24
Shear modulus (Pa)	430	610	400
Density (Kg/m ³)	3200	1456	3900

then fitted to a circle by the least square method. The correspondence relationship K1 between the true value and pixel value of the calibration plate is obtained by the function IMAQ Calibration Target to Points - Circular Dots VI to. Then, the tool edge profile image is calibrated by function IMAQ Set Calibration Info VI, through which the actual value of the tool edge radius is obtained. The prepared tool edge parameter detection system interface is shown in Figure 7. The prepared tool edge radius is detected accurately.

Experimental results and analysis

In order to verify the correctness of the mathematical model of the cutting tool edge radius and the validity of the detection system, the edge preparation experiment was conducted by the drag finishing method. The experimental setup was as follows.

1. Equipment: The drag finishing equipment, shown in Figure 1, was chosen for edge preparation.
2. Tools: The ZX40 tool was used as a cemented carbide milling tool. The rake was 14°, and the relief angle was 15°. The edge length was 25 mm, the diameter was 10 mm, and the total length was 75 mm.
3. Abrasive particles: The abrasive particles consisted of silicon carbide and brown alumina; their parameters are summarized in Table 1.
4. Barrel size: The barrel radius was 200 mm, and the height was 500 mm.
5. Edge radius detection equipment: The high-resolution thermal field emission scanning electron microscope Zeiss SUPRA40 made in Germany was used to measure the edge radius.

The experiment included two factors and three levels, in which the edge preparation speed was set to 20 r/min, 30 r/min, and 40 r/min, respectively; and the edge preparation time was set to 15 min, 30 min, and 45 min, respectively. The drag finishing was used for edge preparation. The test and analytical results obtained using the above-presented mathematical model, the detection system, and the scanning electron microscope (SEM) are given in Table 2. The comparisons of the edge radius are shown in Figures 8–10.

As presented in Table 2, the maximum error between the theoretical value and the measured value of the edge radius was 11.18 μm while the minimum error was 0.07 μm. As seen from the figures, with the increase in the edge preparation time, the number of impacts of the silicon carbide abrasive particles on the milling tool

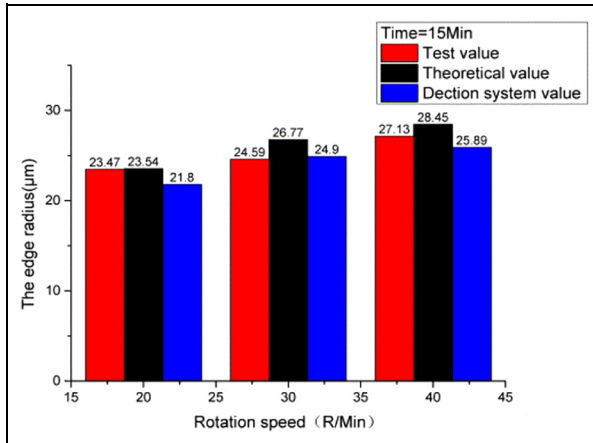


Figure 8. Comparison of the edge radius for the edge preparation time of 15 min.

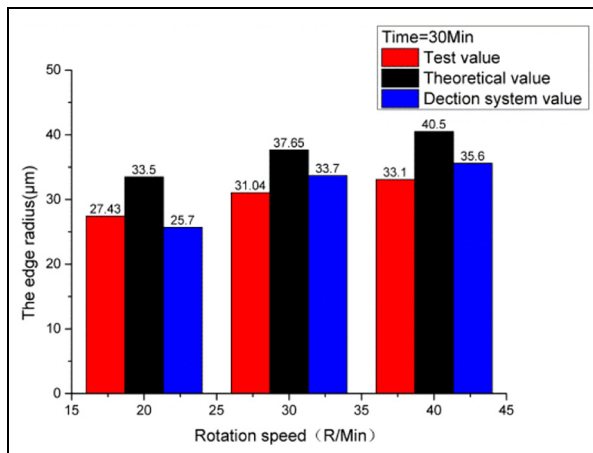


Figure 9. Comparison of the edge radius for the edge preparation time of 30 min.

edge also increased. Therefore, the volume of material removed from the milling tool edge increased with a consequent increase in the edge radius. With the increase in the edge preparation speed, the larger the impact speed of the abrasive particle on the milling tool edge was, the greater the kinetic energy of the abrasive particles was. The larger the amount of material removed from the milling tool edge was, the greater the edge radius was. Therefore, with the increase in the edge preparation time and speed, the edge radii obtained analytically as well as those obtained by the SEM measurement showed an increasing trend. In fact, the abrasive particles were not strictly spherical. The loss in the impact kinetic energy of the abrasive particles was not completely used for material removal. Therefore, although there was a

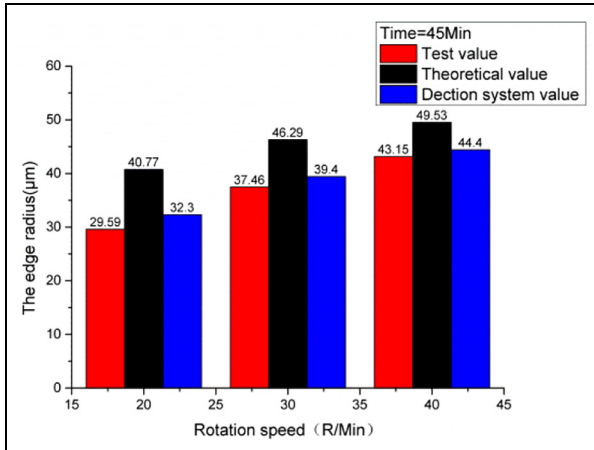


Figure 10. Comparison of the edge radius for the edge preparation time of 45 min.

certain error between the theoretical and experimental values of the cutting tool edge radius, the variation trends of the theoretical and measured values matched closely as can be understood. So, the mathematical modeling method of the edge radius can be considered valid.

It can be seen from the table that the maximum difference between the detection value of the scanning electron microscope (SEM) and the edge detection system is $2.71 \mu\text{m}$, and the minimum difference is $0.31 \mu\text{m}$. The maximum difference percentage between this system and the SEM test is 9.2%, and the minimum difference percentage is 1.2%.

Conclusions

In this paper, a mathematical model of the milling tool motion trajectory is developed based on the characteristics of the drag finishing operation used for edge preparation. Subsequently, the material removal model of a single abrasive particle on the cutting tool edge is designed based on the energy conservation principle and energy absorption theory. On this premise, the mathematical models of the action of multiple abrasive particles on the tool edge and edge radius are proposed using statistical and geometric methods, respectively. The machine vision technology is introduced into the prepared tool edge detection. Based on the basic principle of the machine vision, according to the tool edge preparation characteristics, the prepared tool micron-level edge detection method is proposed. The histogram specification method, median filtering, multi-threshold segmentation method, and Canny edge detection operator are adopted to obtain the edge contour. The micro-level edge detection method is tested by comparison with the theoretic and SEM results. The comparison results lay a foundation for optimization of the edge preparation process and realization of high-speed and high-efficiency cutting.

Table 2. Comparison of the SEM-measured, theoretical, and detection values of edge radius.

No	Speed (r/min)	Time (min)	Edge radius (μm)				SEM value (μm)	Modeling value (μm)	Error (μm)	Error (%)	Detection value	Error (μm)	Error (%)
			No.1 edge	No.2 edge	No.3 edge	No.4 edge							
1	40	15	25.24	-	27.13	29.03	27.13	28.45	1.32	4.8%	25.89	2.56	4.5%
2	40	30	36.62	30.15	34.61	31.04	33.10	40.50	7.4	22.3%	35.6	2.5	7.5%
3	40	45	40.2	44.33	44.1	43.99	43.15	49.53	6.38	14.8%	44.4	1.25	2.8%
4	30	15	24.01	24.54	26.24	23.56	24.59	26.77	2.18	8.8%	24.9	0.31	1.2%
5	30	30	32.94	32.49	29.03	29.7	31.04	37.65	6.61	21.2%	33.7	2.66	8.6%
6	30	45	38.19	40.75	39.41	31.49	37.46	46.29	8.83	25.3%	39.4	1.94	5.2%
7	20	15	23.67	22.11	24.68	23.45	23.47	23.54	0.07	0.2%	21.8	1.67	7.1%
8	20	30	29.25	26.91	26.13	-	27.43	33.50	6.07	22.1%	25.7	1.73	6.3%
9	20	45	28.70	-	31.49	28.58	29.59	40.77	11.18	31.7%	32.3	2.71	9.2%

The main conclusions are as follows.

1. The edge preparation mechanisms of a single particle and multiple particles on the tool edge are explained. A mathematical model of the edge radius is established, which provides a basis for a deeper understanding of the edge preparation effect.
2. The tool edge is prepared by the drag finishing method. Comparison and analysis of the edge radii measured by the SEM and calculated by the proposed model are conducted. The results show that with the increase in the edge preparation speed and time, the edge radius increases. The maximum error between the analytical results and SEM measurements is $11.18\ \mu\text{m}$, while the minimum error is $0.07\ \mu\text{m}$, which verifies the correctness of the mathematical model and the feasibility of the method.
3. The maximum difference between the two methods is $2.71\ \mu\text{m}$, and the minimum difference is $0.31\ \mu\text{m}$. The maximum difference in percentage is 9.2%, and the minimum difference in percentage is 1.2%. The accuracy and feasibility of the proposed prepared tool edge detection system are verified, which provides the basis for further research on the tool edge preparation and realization of high-speed and high-efficient machining.


Declaration of conflicting interests

The author(s) declared no potential conflicts of interest with respect to the research, authorship, and/or publication of this article.

Funding

The author(s) disclosed receipt of the following financial support for the research, authorship, and/or publication of this article: The work presented in this paper was supported by the National Natural Science Foundation Project (No.51665007) and the Research Fund of High-Level Innovative Talents Project in Guizhou Province (Grant No.[2018]190).

ORCID iD

Zhao Xuefeng  <https://orcid.org/0000-0002-2883-8441>

References

1. Bogdan BM, Sabin PM, Stefan S, et al. Unconventional technologies in preparation of microgeometry edges on cutting tools. *Nonconv Technol* 2013; 12: 10–16.
2. Uhlmann E, Eulitz A and Dethlefs A. Discrete element modelling of drag finishing. *Procedia Cirp* 2015; 31: 369–374.
3. Ratia V, Miettunen I and Kuokkala VT. Surface deformation of steels in impact-abrasion: the effect of sample angle and test duration. *Wear* 2013; 301: 94–101.
4. Kumar N and Shukla M. Finite element analysis of multi-particle impact on erosion in abrasive water jet machining of titanium alloy. *J Comput Appl Math* 2012; 236: 4600–4610.

5. Agbaraji C and Raman S. Basic observations in the flat lapping of aluminum and steels using standard abrasives. *Int J Adv Manuf Technol* 2009; 44: 293–305.
6. Sankar MR, Jain VK and Ramkumar J. Rotational abrasive flow finishing (R-AFF) process and its effects on finished surface topography. *Int J Mach Tools Manu* 2010; 50: 637–650.
7. Qian Fa, Ju D, Long Y and Bing Hai L. Fixed abrasive tool characteristics on tool wear and material removal in processing. *Nanotechnol Precis Eng* 2012; 10(1): 89–94.
8. Uhlmann E, Eulitz A and Dethlefs A. Discrete element modelling of drag finishing. *Procedia Cirp* 2015; 31: 369–374.
9. Barletta M, Gisario A, Venettacci S, et al. A comparative evaluation of fluidized bed assisted drag finishing and centrifugal disk dry finishing. *Eng Sci Technol Int J* 2014; 17(2): 63–72.
10. Sooraj VS and Radhakrishnan V. A study on fine finishing of hard workpiece surfaces using fluidized elastic abrasives. *Int J Adv Manuf Technol* 2014; 73(9–12): 1495–1509.
11. Yeong LT and Ratnam MM. Measurement of nose radii of multiple cutting tool inserts from scanned images using sub-pixel edge detection. In: *13th International Conference on Control Automation Robotics & Vision (ICARCV)*, Singapore, 10–12 December 2014. IEEE. pp. 100–105.
12. Lim TY and Ratnam MM. Edge detection and measurement of nose radii of cutting tool inserts from scanned 2-D images. *Opt Lasers Eng* 2012; 50(11): 1628–1642.
13. Chian GJ and Ratnam MM. Determination of tool nose radii of cutting inserts using machine vision. *Sens Rev* 2011; 31(2): 127–137.
14. Shahabi HH. Simulation and measurement of surface roughness via grey scale image of tool in finish turning. *Precis Eng* 2016; 43: 146–153.
15. Barletta M, Rubino G and Valentini PP. Experimental investigation and modelling of fluidized bed assisted drag finishing according to the theory of localization of plastic deformation and energy absorption. *Int J Adv Manuf Technol* 2014; 12: 1–16.
16. Mehrabia A, Mehrshada N and Massinaei M. Machine vision based monitoring of an industrial flotation cell in an iron flotation plant. *Int J Miner Process* 2014; 133: 60–66.
17. Biswas R and Sil J. An improved canny edge detection algorithm based on type-2 fuzzy sets. *Proc Technol* 2012; 4: 820–824.

Author biographies

Zhao Xuefeng is a Professor at Guizhou University. Her academic research interest is in the field of advanced processing and manufacturing technique.

Li Hui is a Postgraduate at Guizhou University. His academic research interest is in the field of Edge preparation technique.

He Lin is a Professor at Guizhou University. His academic research interest is in the field of tool design and manufacture method.

Tao Meng is a Professor at Guizhou University. His academic research interest is in the field of noise and vibration control technique.